

Influence of In doping on electro-optical properties of ZnO films

A P RAMBU*, D SIRBU, A V SANDU†, G PRODAN†† and V NICA

Alexandru Ioan Cuza University of Iasi, University of Iasi, Faculty of Physics, 11 Carol I Blvd., Iasi 700506, Romania

†Gheorghe Asachi Tech University, Faculty of Materials Science & Engineering, Iasi 700050, Romania

††“Ovidius”, University of Constanta, Bd. Mamaia 124, Constanta, Romania

MS received 1 March 2012; revised 30 April 2012

Abstract. Thin metallic films of Zn and In/Zn were deposited onto glass substrates by thermal evaporation under vacuum. The metallic films were submitted to a thermal oxidation in air, at 623 K, for different oxidation times (30–90 min), in order to be oxidized. Structural and morphological analyses (X-ray diffraction, transmission electron microscopy and scanning electron microscopy) revealed that the obtained undoped and In-doped ZnO thin films possess a polycrystalline structure. Transmission spectra were recorded in spectral domain from 280 to 1400 nm. The influence of In doping and oxidation parameters as well, on the optical parameters (transmittance, optical bandgap, Urbach energy) were analysed. It was clearly evidenced that by In doping, the optical properties of ZnO films were improved. The temperature dependence of electrical conductivity was studied using surface-type cells with Ag electrodes. The obtained results indicate that In-doped ZnO films exhibit an enhancement of electrical conductivity with few orders of magnitude when compared with non-doped ones.

Keywords. Doped-zinc oxide; microstructure; optical parameters; electrical conductivity.

1. Introduction

ZnO can be considered as an “old” semiconductor which has attracted researcher’s attention for a long time because of its large area of applications. Zinc oxide is a direct bandgap semiconductor with $E_g = 3.37$ eV (at room temperature) having hexagonal (wurtzite) structure with lattice parameters $a = 0.325$ nm and $c = 0.512$ nm (Jagadish and Pearton 2006). Stoichiometric films are insulating whereas nonstoichiometric and oxygen deficient films are very good as transparent semiconducting oxides.

Transparent conducting oxides (TCO’s) in thin films have become very important for a variety of applications including gas sensors (Ferro *et al* 2008), optoelectronic devices (Shinde *et al* 2008), organic solar cells (Kyaw *et al* 2011) and others. Zinc oxide (ZnO) thin films present a particular importance due to their great optical transmittance in the visible wavelength range. Unfortunately, undoped-ZnO films have poor electrical conductivity. It was experimentally established that, by doping with 3rd group elements (Al, In, Ga), we can prepare ZnO films having a higher electrical conductivity and a better optical transmittance in visible region in comparison with non-doped films. These dopants (In^{3+} , Al^{3+} and Ga^{3+}) act as a donor when it occupies a substitutional position for Zn^{2+} or an interstitial position in the ZnO lattice. Regarding the electrical resistivity of doped-ZnO thin

films, values of 10^{-4} ($\Omega^{-1} \times \text{cm}^{-1}$) were reported (Wong *et al* 2011).

On the other hand, the deposition method and deposition parameters are influencing the structural properties of the films and consequently, the electrical and optical ones. Therefore, apart from dopant nature and concentration, the deposition method and parameters must be optimized such that the obtained films to possess the desired properties.

Various deposition techniques were employed to obtain doped-ZnO thick and thin films and the dependences of the physical properties on the deposition parameters were discussed. Therefore, indium-doped zinc oxide thin films can be obtained by various deposition techniques including spray pyrolysis technique (Shinde *et al* 2008), sol-gel technique (Kyaw *et al* 2011), electrodeposition (Machado *et al* 2005), pulsed laser deposition (Kotlyarchuk *et al* 2005), d.c. magnetron sputtering (Park *et al* 2009), etc.

The films analysed in this paper are obtained by thermal oxidation of metallic films. The main goal of this study is to investigate the influence of oxidation parameters on optical and electrical properties of In-doped ZnO films.

In a previous work (Rusu *et al* 2008), we reported some results on the optical and electrical properties of In-doped ZnO prepared by thermal oxidation of multilayered Zn/In thin films.

2. Experimental

Thermal oxidation of metallic films represents a simple and low cost method which allow to obtain oxide thin films. Of

*Author for correspondence (alicia.rambu@uaic.ro)

course, the properties of so-obtained films will depend on the deposition parameters used for the deposition of metallic films and also on the oxidation parameters.

Zn and In/Zn, with weight ratios of 0.03, metallic films were obtained by thermal evaporation under vacuum. The metallic films were deposited onto properly cleaned glass substrates with typical size of 10 mm × 10 mm × 1 mm. The thin films under study were prepared using the following deposition parameters: evaporator (source)–substrate distance was 8 cm; substrate temperature was 300 K and vacuum pressure was 4×10^{-5} torr. The source materials were zinc and indium metal (in the form of pellets) with a purity of 99.9%.

The oxidation procedure consists of the following succession of technological runs: a heating (in the temperature range from 300 to 623 K), with a heating rate of about 6 K/min; an annealing for a certain oxidation time, ($t = 30, 60$ and 90 min) at an oxidation temperature; a cooling from oxidation temperature to room temperature.

Table 1 presents the deposition parameters and sample codes.

The crystalline structure of undoped and In-doped ZnO films was investigated by means of X-ray diffraction, using a Shimadzu LabX XRD-6000 diffractometer with $\text{CuK}\alpha$ radiation ($\lambda = 1.5408 \text{ \AA}$). Transmission electron microscopy (TEM) investigations were performed with a Philips CM 120 ($\lambda = 0.037 \text{ \AA}$), operated at 100 kV, having a resolution of 4 \AA .

The surface morphology of investigated films was examined using a scanning electron microscopy (SEM), model Vega II LSH.

Transmission spectra were recorded, using a computer-controlled UV–Vis–NIR spectrometer type Tech5 AG. A blank glass substrate was used as reference for transmittance measurements.

The temperature dependence of electrical conductivity was investigated using surface-type cells. Silver electrodes were deposited by thermal evaporation under vacuum after the oxidation process. The temperature dependence of the electrical conductivity was investigated during a heat treatment consisting of two heating and cooling cycles in a temperature range $\Delta T = 300\text{--}473 \text{ K}$. The electrical measurements were performed in a two-point's configuration, by using a sensitive Keithley model 6517 multimeter.

Table 1. Deposition parameters.

Sample	Material	T (K)	t (min)	r (K/min)
Z.1	ZnO	623	30	6
Z.2	ZnO		60	
Z.3	ZnO		90	
Z.I.1	ZnO:In		30	
Z.I.2	ZnO:In		60	
Z.I.3	ZnO:In		90	

T , oxidation temperature; t , oxidation time and r , heating rate.

3. Results and discussion

3.1 Microstructural analyses

Characteristic XRD patterns of undoped and doped-ZnO films are presented in figure 1. Diffraction peaks from ZnO characteristic diffractogram were assigned to be hexagonal (wurtzite) ZnO based on comparison with JCPDS card (Joint Committee Power Diffraction Standards). No characteristic peak of Zn metal was observed, indicating complete oxidation of zinc film. It is significant to note that in the case of In-doped ZnO, no traces of the dopant or its respective oxides were observed by means of X-ray diffraction. The absence of metal XRD peaks indicates that simultaneously with zinc oxidation during thermal annealing, a diffusion of In atoms newly formed ZnO lattice takes place. In atoms are incorporated in interstitial positions in ZnO lattice or as substitutional ions in Zn site.

Also, it can be observed that both undoped and doped films have a preferential orientation with (002) planes parallel to the substrate. The other peaks observed in the X-ray diffractograms are (100) and (101) but intensity of these peaks are found to be too less as compared to the preferentially oriented peak.

TEM analyses were carried out indicating the crystalline nature of the analysed films. Low-magnification TEM micrographs characteristic for ZnO and In:ZnO (figures 2(a) and (b)) exhibit that the analysed films are crystalline and the

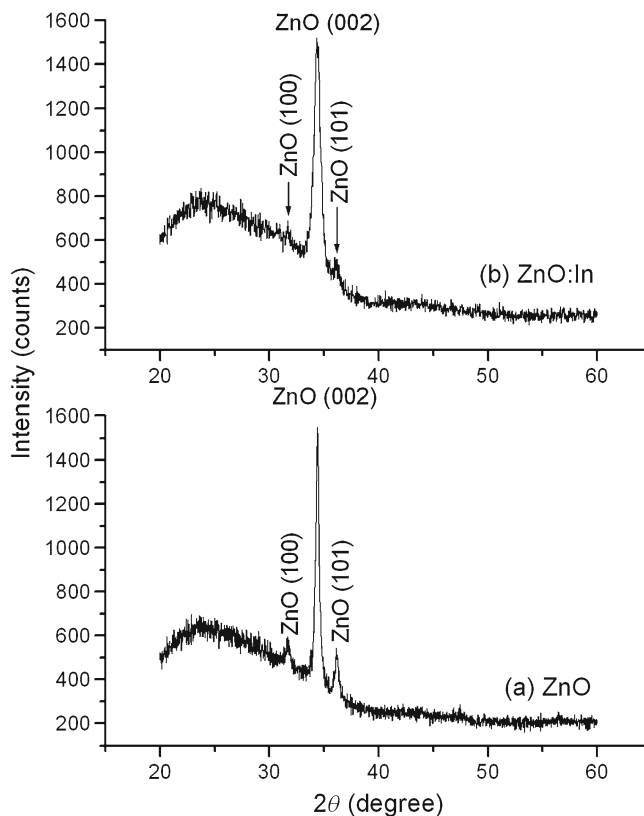


Figure 1. XRD patterns for (a) ZnO and (b) ZnO:In samples.

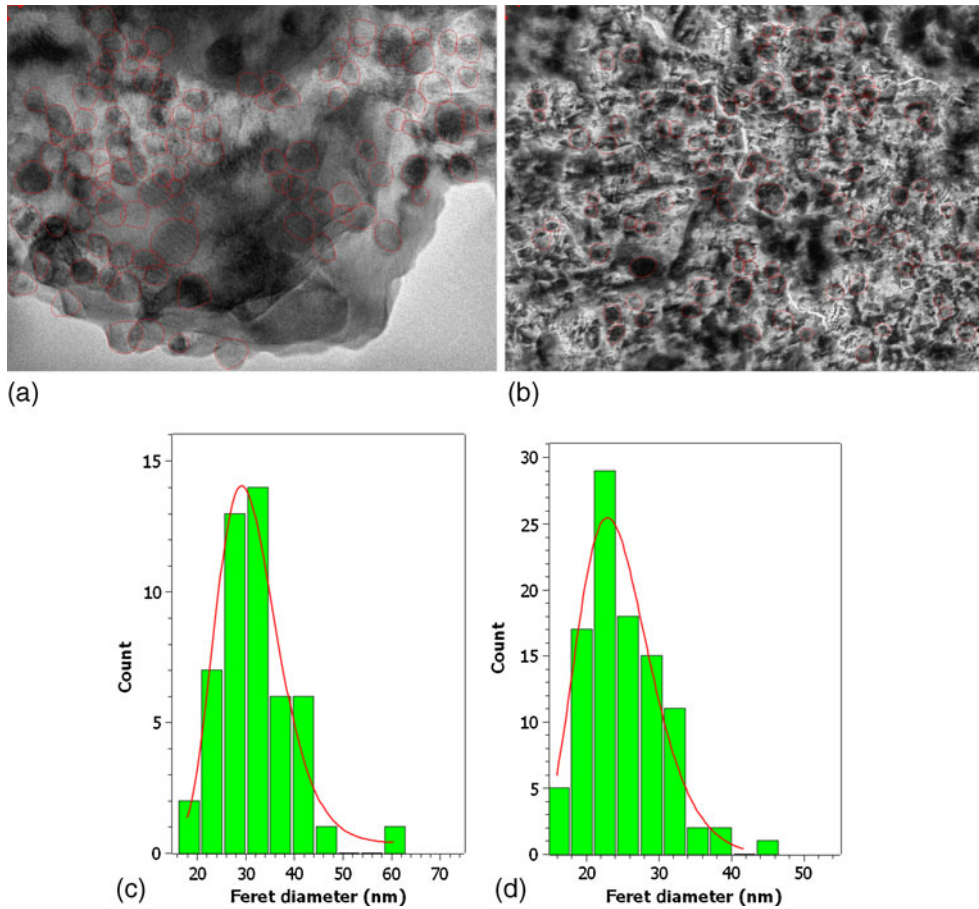


Figure 2. TEM images of (a) ZnO and (b) ZnO:In samples. Histograms of (c) ZnO and (d) ZnO:In samples.

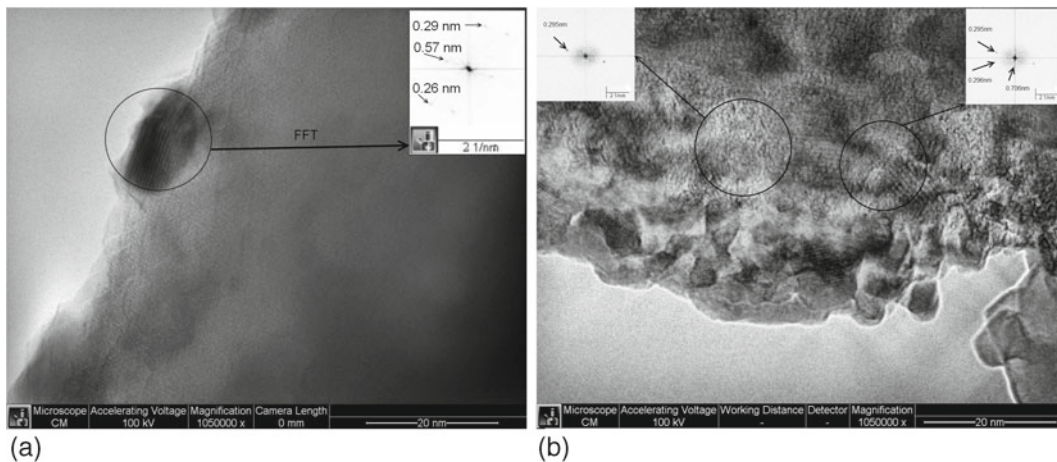


Figure 3. Characteristic HRTEM images for (a) ZnO and (b) ZnO:In samples.

crystallites formed agglomerations with polyhedral shapes. The particle diameter is evaluated by mean value of the distances between pairs of parallel tangents and the projected outline of the particle (Feret's diameter) (Walton 1948; Kohli and Mittal 2012). The mean diameter is calculated assuming a log-normal distribution of experimental data. The his-

togram grain size distribution is shown in figures 2(c) and (d). It can be seen, from the characteristic histograms, that the mean grain size for ZnO is about 29 nm and for In-doped ZnO, it is decreasing to about 24 nm.

HRTEM analysis provides the structure of thin films in detail. Figure 3(a) presents the characteristic HRTEM image

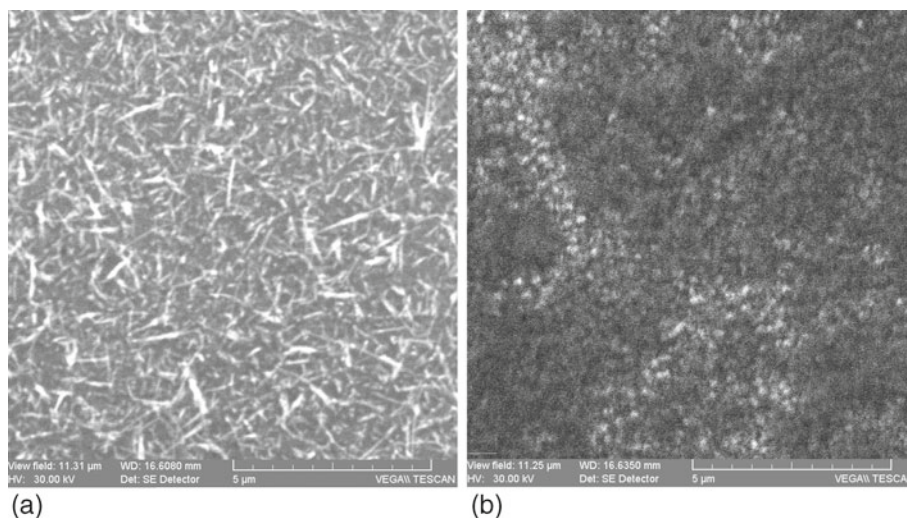


Figure 4. SEM characteristic micrographs of (a) ZnO and (b) ZnO:In samples.

for Z.1 sample. This image reveal lattice fringes with interlayer distances of 0.29 and 0.26 nm, respectively ascribable to zinc oxide (100) and (002) planes, respectively. Figure 3(b) presents HRTEM image characteristic for ZI.1 sample and in this case lattice fringes with interlayer distances of 0.295 nm, corresponding to (100) planes, were identified.

Surface morphology was observed by scanning electron microscopy (SEM). SEM micrographs reveal that the undoped and In-doped ZnO possess different features: a coarser surface is obtained for the undoped films and a surface composed of regular and round grains is observed in the case of ZnO:In films (figure 4).

Surface morphology changes induced by doping were reported by others. For example, Lupan *et al* (2009) reported that Al-doping allows in obtaining more dense films, with higher surface-to-volume ratio by comparison with non-doped ZnO films. They concluded that Al doping leads to the changes in film structure. Shinde *et al* (2008) reported that in the ZnO film with 3 at% indium doping presents a nanocrystalline surface smoother than that of pure ZnO, and the grain size of doped film being smaller than that of pure ZnO film.

3.2 Optical properties

In order to analyse the effect of the doping on the transparency and the bandgap energy of the films, optical transmittance spectra were recorded for all deposited films. The optical transmittance, corrected from the effect of glass substrate, was plotted in spectral domain (280–1400) nm. The optical transmission spectra of undoped-ZnO films, presented in figure 5(a), shows that the studied films have a high transmission coefficient in the visible and near-infrared range. In the visible domain, maximum transmittance is ranged between 85 and 90%. It can be observed, from the characteristic plots, that the optical transmittance is decreasing once the oxidation time is increasing. This kind of

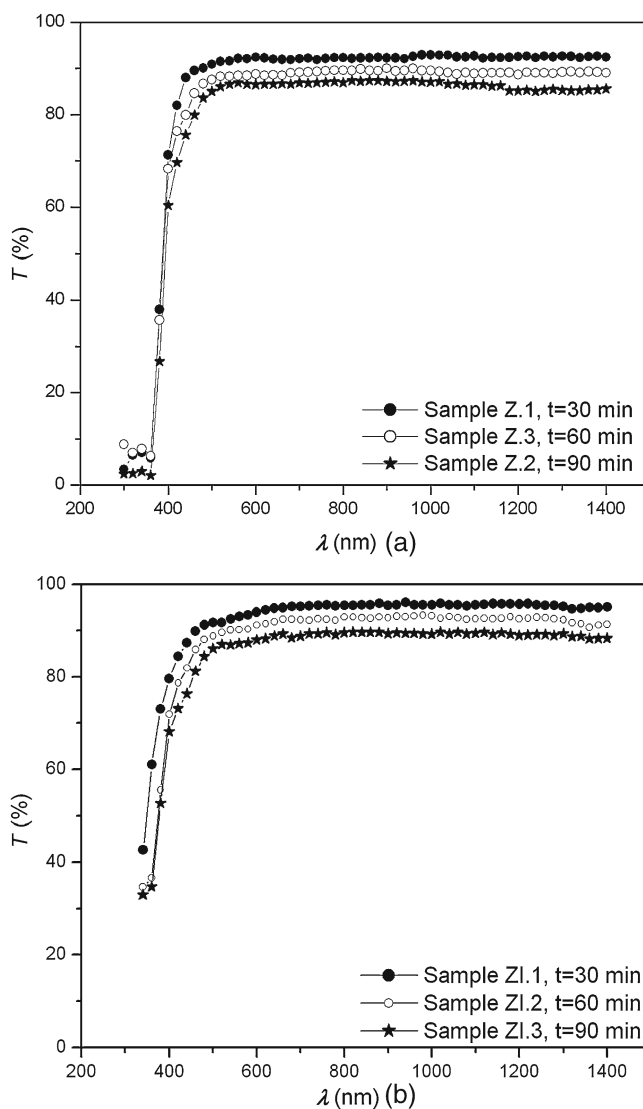


Figure 5. Optical transmittance spectra of (a) undoped-ZnO and (b) In-doped ZnO films.

behaviour was observed before and it was explained by the deterioration of the structure with the increase in oxidation time (Rambu and Rusu 2010). An increase of transmittance is observed for In-doped films, by comparison with non-doped ones. Therefore, in the case of doped films, the optical transmittance is ranged between 88 and 95%, in visible domain. The increase in transmittance for doped films can be correlated with their better crystallinity. This assumption is in accordance with the results reported by Ramamoorthy *et al* (2006), which revealed that the ZnO films, deposited by pulsed-laser deposition, with textured and better aligned microstructure have superior transmission to randomly oriented and an improved electrical conductivity.

Generally, the optical transmittance of the thin films may be influenced by different factors: film thickness, structural defects, surface roughness, presence of mixed phases, etc (Song *et al* 2004; Luna-Arredondo *et al* 2005). Therefore, we presume that higher optical transmittances were obtained for doped films because of improved structure and different morphologies (see figure 4).

It can be observed that all samples are characterized by a sharp absorption edge and a constant higher transmittance values in all the wavelength range 400–1400 nm.

The short wavelength cut-off in the transmission below 400 nm is due to the fundamental bandgap excitation from the valence band to the conduction band. Energy bandgap of studied samples has been evaluated from absorption spectra. ZnO is considered to be a direct gap material. Consequently, the absorption coefficient can be described by the expression (Hodgson 1970; Moss *et al* 1973):

$$\alpha = \left(\frac{A}{h\nu} \right) (h\nu - E_g)^{1/2}, \quad (1)$$

where $h\nu$ is photon energy, E_g the direct optical bandgap and A the characteristic parameter for respective transitions.

According to the above relation, the dependence $(\alpha h\nu)^2 = f(h\nu)$ must be linear, supposing that parameter A does not depend on the photon energy. By extrapolating the linear region portions of $(\alpha h\nu)^2 = f(h\nu)$ curves to $(\alpha h\nu)^2 = 0$, the values of direct optical bandgap have been determined.

An increase in E_g values was observed, for doped films when compared with non-doped films.

Generally, the conduction characteristics of ZnO films are dominated by electrons generated from oxygen vacancies and zinc interstitial atoms, which determine the shift of optical bandgap to values lower than 3.37 eV. It was observed that for indium-doped films, some values of optical bandgap are larger than 3.37 eV. It is supposed that the contribution from In^{3+} ions on substitutional sites of Zn^{2+} ions and In-interstitial atoms determine the widening of the bandgap caused by increase in carrier concentration (Joseph *et al* 2005; Singh *et al* 2010). The Burstein–Moss effect explained the broadening of bandgap energy with the increase in carrier concentration.

The absorption coefficient near fundamental absorption edge, in the energy region of $h\nu < E_g$, obeys the empirical Urbach relation (Tauc 1974):

$$\alpha = \alpha_0 \exp\left(\frac{h\nu - E_U}{E_U}\right), \quad (2)$$

where E_U is Urbach energy, E_U and α_0 are constants.

Equation (2) describes the optical transition between occupied states in the valence band tail to unoccupied states of the conduction band edge. The appearance of Urbach tail is due to the structure disorder, caused by the defects and doping in

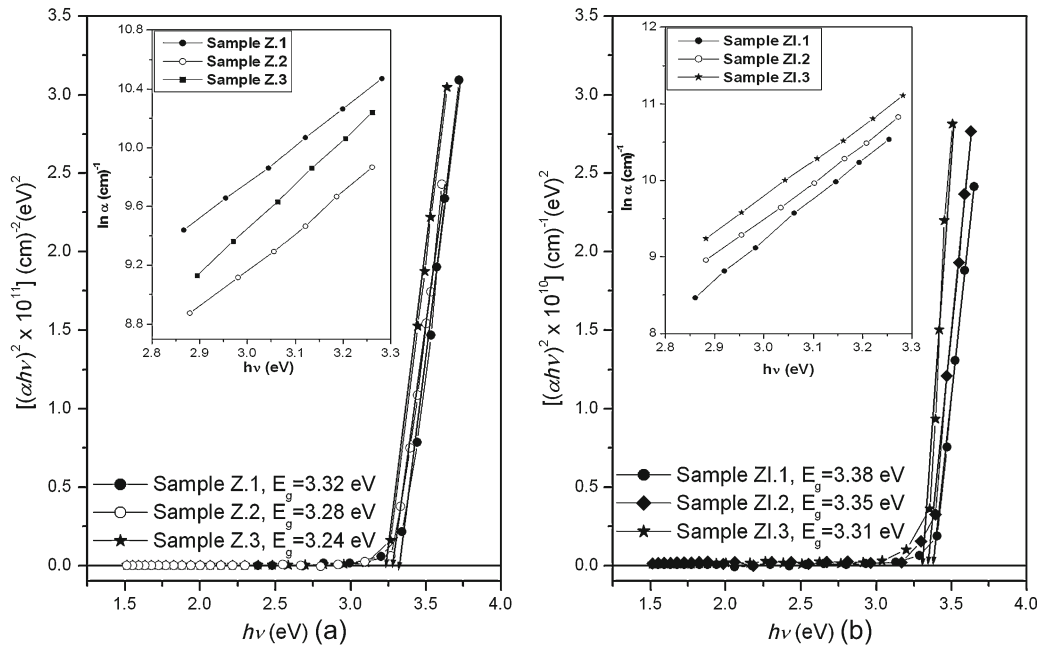


Figure 6. $(\alpha h\nu)^2 = f(h\nu)$ dependences of (a) ZnO and (b) ZnO:In films (Insets are presented with $\ln \alpha = f(h\nu)$ dependences).

the thin films (Caglar *et al* 2009). Taking into account relation (2), a plot of $\ln \alpha = f(h\nu)$ should be linear and Urbach energy can be obtained from the slope.

Inset graphs of figures 6(a) and (b) show the variation of $\ln \alpha$ vs photon energy for the ZnO and In:ZnO films. The calculated values of optical bandgap and Urbach energy are listed in table 2. As it can be observed, the values of E_U calculated for doped samples are larger than those of non-doped films, because In replaces Zn in the lattice structure partly inducing structure disorder. Also, it may be seen that once the oxidation time is increased, the E_U value increases and E_g value decreases. The increase of E_U suggests that the atomic structural disorder of studied films increase and may explain the decrease of optical transmittance with increasing oxidation time (see figure 5).

Similar results are obtained by Mamat *et al* (2009) for Al-doped ZnO films. For doped films, the values of energy bandgap and Urbach energy are larger than those obtained for non-doped films. Caglar *et al* (2009) analysed the effect of indium incorporation on structural and optical properties of ZnO films. They obtained higher values of Urbach energy for doped films by comparing with non-doped ones and these values are increasing with increase in doping concentration.

3.3 Electrical conductivity

It was experimentally established that thin films with stable structure can be obtained if they, after preparation, were subjected to a heat treatment. In the same time, it must be mentioned that there is a strong correlation between structural characteristics of a thin film and its electrical properties. Consequently, the variation of electrical conductivity during two successive heating–cooling cycles within the temperature range $\Delta T = 300$ –473 K was recorded.

It is supposed that a heat treatment leads to the removal of the adsorbed and/or absorbed gases, a reduction in the concentration of the structural defects, increasing grain size and consequently decreasing grain boundary, therefore, by applying a heat treatment, the electrical conductivity may be improved (Hamad *et al* 2005; Raoufi and Raoufi 2009).

The variation of electrical resistance was measured with film temperature up to 473 K, the same dependences are

Table 2. Calculated values of some characteristic parameters.

Sample	T (K)	t (min)	E_g (eV)	E_U (eV)	σ ($\Omega \times \text{cm}$) ⁻¹
Z.1	623	30	3.32	0.25	4.12×10^{-3}
Z.2		60	3.28	0.26	1.84×10^{-3}
Z.3		90	3.24	0.30	1.02×10^{-3}
ZI.1		30	3.38	0.46	4.26
ZI.2		60	3.35	0.48	2.18
ZI.3		90	3.31	0.52	1.17

T , oxidation temperature; t , oxidation time; E_g , optical bandgap; E_U , Urbach energy and σ , electrical conductivity at room temperature.

recorded during the cooling as well. Once it reached the room temperature, the films were subjected to a second heating–cooling cycle. The $\ln \sigma = f(10^3/T)$ dependences, for second cooling, are presented in figure 7. For undoped ZnO films, the values of electrical conductivities were found to be ranged between 1.02×10^{-3} ($\Omega \times \text{cm}$)⁻¹ and 3.12×10^{-3} ($\Omega \times \text{cm}$)⁻¹. It was expected to obtain such lower values for electrical conductivity, because as we mentioned before, undoped-zinc oxide films are highly resistive. But these values are in good agreement with those reported before (Rusu *et al* 2007, 2008; Rambu *et al* 2012). A small decrease of electrical conductivity with increase in oxidation temperature is observed. This behaviour may be due to the fact that oxygen vacancies are decreasing once the oxidation time is increased. Probably an oxidation time of 30 min does not produce the complete oxidation of metal substance. So, by increasing the oxidation time, the oxidation process

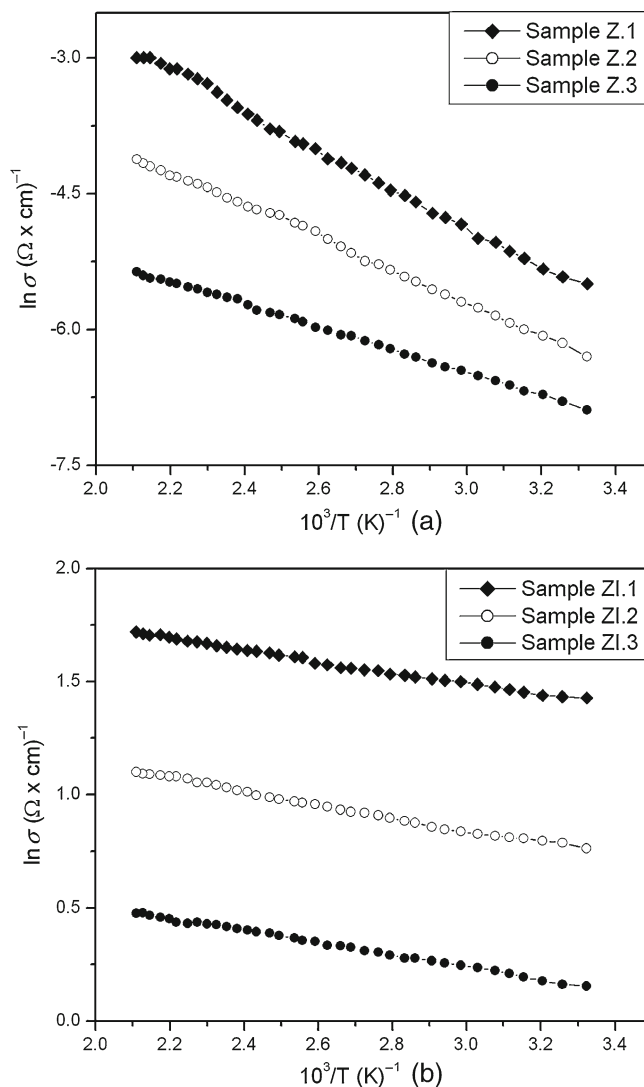


Figure 7. $\ln \sigma = f(10^3/T)$ dependences for (a) ZnO thin films and (b) In-doped ZnO films.

continues, a decrease in the oxygen vacancies takes place and consequently, the values of electrical conductivity is decreased.

It was seen that by In doping, the electrical conductivity increases, values ranged between $1.16 (\Omega \times \text{cm})^{-1}$ and $4.15 (\Omega \times \text{cm})^{-1}$ are obtained. As it can be observed, the electrical conductivity of ZnO:In thin films is increased with few orders of magnitude by comparing with the conductivity of non-doped ZnO films. Such behaviour was observed and reported before (Rusu *et al* 2008; Singh *et al* 2010). It is well known that a high electrical conductivity is archived in a semiconducting oxide due to high electron concentration resulting from deviation from stoichiometry or impurity doping effects. When a third group element, In, in this case, is introduced in ZnO lattices, In^{3+} atoms substitute Zn^{2+} atoms and act as donors. An increase in the electrical conductivity by In doping, can be attributed to the optimal incorporation of indium atoms in ZnO lattice, increasing the donor concentration.

4. Conclusions

The electro-optical properties of ZnO and In-doped ZnO films were investigated. Polycrystalline undoped and In-doped ZnO films were obtained by thermal oxidation of vacuum evaporated metallic films. The obtained films possess a hexagonal (wurtzite) structure and the crystallites are preferentially oriented with the (002) planes parallel to the substrate. It is observed that the doping with In in ZnO showed conductivity enhancement along with improved transparency.

Optical parameters (transmittance, optical bandgap and Urbach energy) are larger for doped films when compared with non-doped ones and tend to decrease with increasing oxidation time. The electrical conductivity of ZnO films increases with few orders of magnitude when In is incorporated in ZnO lattice.

References

- Caglar M, Ilican S and Caglar Y 2009 *Thin Solid Films* **517** 5023
 Ferro R, Rodríguez J A and Bertrand P 2008 *Thin Solid Films* **516** 2225
 Hamad O, Braunstein G, Patil H and Dhere N 2005 *Thin Solid Films* **489** 303
 Hodgson J N 1970 *Optical absorption and dispersion in solids* (London: Chapman and Hall)
 Jagadish C and Pearton S J 2006 *Zinc oxide bulk, thin films and nanostructures: processing, properties and applications* (Amsterdam: Elsevier)
 Joint Committee on Powder Diffraction Standards, Powder Diffraction File, International Center for Diffraction Data, Swarthmore, PA, 1997, card 36-1451
 Joseph B, Manoj P K and Vaidyan V K 2005 *Bull. Mater. Sci.* **28** 487
 Kohli R and Mittal K L 2012 *Developments in surface contamination and cleaning – detection, characterization, and analyses of contaminants* (Amsterdam: Elsevier)
 Kotlyarchuk B, Savchuk V and Oszwaldowski M 2005 *Cryst. Res. Technol.* **40** 1118
 Kyaw A K K, Wang Y, Zhao D W, Huang Z H, Zeng X T and Sun X W 2011 *Phys. Status Solidi A* **208** 1
 Luna-Arredondo E J, Maldonado A, Asomoza R, Acosta D R, Melendez-Lira M A and de la Olvera L M 2005 *Thin Solid Films* **490** 132
 Lupan O *et al* 2009 *Mater. Res. Bull.* **44** 63
 Mamat M H, Sahdat M Z, Amizam S, Rafeie H A, Khusaimi Z and Rusop M 2009 *J. Ceram. Soc. Jpn.* **117** 1263
 Machado G, Guerra D N, Leinen D, Ramos-Barrado J R, Marotti R E and Dalchiele E A 2005 *Thin Solid Films* **490** 124
 Moss T S, Burell G and Ellias G T B 1973 *Semiconductor optoelectronics* (New York: Wiley)
 Park Y R, Jung D, Kim K C, Suh S J, Park T S and Kim Y S 2009 *J. Electroceram.* **23** 536
 Ramamoorthy K, Sanjeeviraja C, Jayachandran M, Sankaranarayanan K, Misra P and Kukreja L M 2006 *Curr. Appl. Phys.* **6** 103
 Rambu A P and Rusu G I 2010 *Superlatt. Microstr.* **47** 300
 Rambu A P, Iftimie N and Rusu G I 2012 *Mater. Sci. Eng. B* **177** 157
 Raoufi D and Raoufi T 2009 *Appl. Surf. Sci.* **255** 5812
 Rusu G G, Girtan M and Rusu M 2007 *Superlatt. Microstr.* **42** 116
 Rusu G G, Rambu A P and Rusu M 2008 *J. Optoelectron. Adv. Mater.* **10** 339
 Singh G, Shrivastava S B, Jain D, Pandya S, Shripathi T and Ganesan V 2010 *Bull. Mater. Sci.* **33** 581
 Shinde S S, Shinde P S, Bhosale C H and Rajpure K Y 2008 *J. Phys. D: Appl. Phys.* **41** 105109
 Song Y S, Park J K, Kim T W and Chung C W 2004 *Thin Solid Films* **467** 117
 Tauc J 1974 *Amorphous and liquid semiconductors* (New York: Plenum Press)
 Walton W H 1948 *Nature* **162** 329
 Wong L M, Chiam S Y, Huang J Q, Wang S J, Pan J S and Chim W K 2011 *Appl. Phys. Lett.* **98** 022106